

# NJC

Accepted Manuscript



This is an *Accepted Manuscript*, which has been through the Royal Society of Chemistry peer review process and has been accepted for publication.

*Accepted Manuscripts* are published online shortly after acceptance, before technical editing, formatting and proof reading. Using this free service, authors can make their results available to the community, in citable form, before we publish the edited article. We will replace this *Accepted Manuscript* with the edited and formatted *Advance Article* as soon as it is available.

You can find more information about *Accepted Manuscripts* in the [Information for Authors](#).

Please note that technical editing may introduce minor changes to the text and/or graphics, which may alter content. The journal's standard [Terms & Conditions](#) and the [Ethical guidelines](#) still apply. In no event shall the Royal Society of Chemistry be held responsible for any errors or omissions in this *Accepted Manuscript* or any consequences arising from the use of any information it contains.



[www.rsc.org/njc](http://www.rsc.org/njc)

## ARTICLE

# Copper hydrotris(3,5-diphenylpyrazolyl)borate dithiocarbamates: mimicking green copper proteins

Cite this: DOI: 10.1039/x0xx00000x

Received 00th January 2012,  
Accepted 00th January 2012

DOI: 10.1039/x0xx00000x

www.rsc.org/

David J. Harding,<sup>a\*</sup> Wasinee Phonsri,<sup>a</sup> Phimphaka Harding,<sup>a</sup> Jitnapa Sirirak,<sup>a</sup> Yuthana Tangtirungrotechai,<sup>b</sup> Richard D. Webster<sup>c</sup> and Harry Adams<sup>d</sup>

Three novel copper hydrotris(3,5-diphenylpyrazolyl)borate ( $\text{Tp}^{\text{Ph}_2}$ ) dithiocarbamate complexes,  $[\text{Tp}^{\text{Ph}_2}\text{Cu}(\text{dte})]$  ( $\text{dte} = \text{S}_2\text{CNET}_2$  **1**,  $\text{S}_2\text{CNBz}_2$  **2** and  $\text{S}_2\text{CN}(\text{CH}_2)_4$  **3**) have been prepared in a simple one pot reaction by sequential addition of  $\text{KTp}^{\text{Ph}_2}$  and  $\text{Na}(\text{dte})$  to  $\text{CuCl}_2 \cdot 2\text{H}_2\text{O}$ . IR, UV-Vis and ESR spectroscopic studies suggest a mostly  $\kappa^3$  coordinated  $\text{Tp}^{\text{Ph}_2}$  ligand, bidentate dithiocarbamate ligands and therefore, a five coordinate copper centre. Unusually, a  $\kappa^3$  to  $\kappa^2$  isomerisation of the  $\text{Tp}^{\text{Ph}_2}$  ligand is found in solution in **3** and to a lesser extent in **1**. The X-ray crystal structures reveal geometries intermediate between trigonal bipyramidal and square pyramidal depending on the steric bulk of the dithiocarbamate ligand and a long Cu-N bond resulting in an asymmetrically bound  $\text{Tp}^{\text{Ph}_2}$  ligand. Electrochemical studies reveal quasi-reversible one-electron oxidation and reduction to Cu(I) with the reversibility and reduction potential strongly dependent on the dithiocarbamate. DFT calculations reveal a weakly antibonding Cu-S  $\pi^*$  SOMO and a strongly antibonding Cu-S  $\sigma^*$  LUMO consistent with the significant effect of the dithiocarbamate ligand on the electrochemical behaviour of these complexes.

## Introduction

Blue copper proteins are amongst the most widely studied proteins in chemistry.<sup>1-4</sup> They are very efficient electron transfer proteins and play a critical role in many enzymatic processes.<sup>1-4</sup> Two of the most common proteins belonging to this family are plastocyanin and azurin. Both proteins exhibit an intense ligand-to-metal charge transfer band at *ca.* 600 nm making the proteins blue in colour hence their name. In the case of plastocyanin, the copper centre is four coordinate with two histidine ligands, a short Cu-S cysteine bond and a long Cu-S bond to a neutral methionine residue leading to a trigonally distorted tetrahedral centre.<sup>5</sup> In contrast, azurin is five coordinate with an additional glycine residue weakly bound to the Cu centre through a carbonyl oxygen.<sup>6-8</sup> The increase in coordination number results in a distorted trigonal bipyramidal geometry with the histidines and cysteine occupying the trigonal plane and the methionine and glycine axially coordinated. The fact that both of these axial ligands are weakly bound (Cu-S(Met)  $\approx$  3.2 Å, Cu-O(Gly)  $\approx$  2.9 Å) results in a short Cu-S bond (*ca.* 2.1 Å) and is directly responsible for the blue colour of this protein.<sup>6</sup> Indeed, studies on modified azurins have shown that introduction of a better donor in the axial position results in a decrease in the S ( $p_\pi$ )-to- $\text{Cu}^{2+}$  LMCT band

at *ca.* 600 nm and a concomitant increase in a new band at *ca.* 400 nm assigned to a S ( $p_\sigma$ )-to- $\text{Cu}^{2+}$  LMCT band and a change in colour to form so-called green copper proteins.<sup>9-11</sup> This change in colour has been ascribed by Solomon and co-workers to a 'coupled distortion' model.<sup>12</sup> According to the model, distortion at the copper centre towards a more tetragonal structure results in more effective overlap of the  $d_{x^2-y^2}$  orbital with the S  $\sigma$  orbital and consequently a more intense band at *ca.* 400 nm.<sup>13,14</sup> Several green copper proteins are known with the best studied being nitrite reductase.<sup>15</sup>

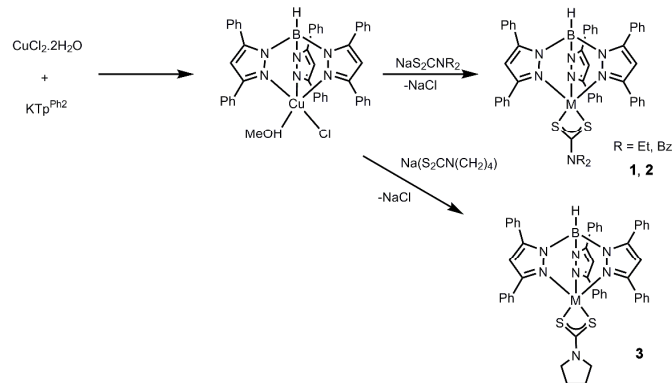
In order to better understand blue copper proteins two families of model complexes have been prepared which closely mimic that of native copper blue enzymes.<sup>16,17</sup> Of particular relevance to the current work are the hydrotris(pyrazolyl)borate series investigated by amongst others Solomon and Fujisawa,  $[\text{Tp}^{\text{R}}\text{CuAr}]$  ( $\text{Tp}^{\text{R}}$  = substituted hydrotris(pyrazolyl)borate; Ar = aryl).<sup>18</sup> Although they possess a  $\text{N}_3\text{S}$  donor set rather than the  $\text{N}_2\text{S}_2$  donor set of the native enzyme one of the pyrazolyl arms is only weakly bound to the Cu centre and thus mirrors that of the methionine donor in plastocyanin.<sup>16,17</sup> The electronic spectral properties also closely resemble those of the enzyme and have provided significant insight into the nature of the Cu-S bond.<sup>18</sup>

Despite the success of  $\text{Tp}^{\text{R}}$  ligands in modeling plastocyanin their use in the modeling of azurin has not been reported to date. We have recently prepared a series of nickel and cobalt dithiocarbamate complexes supported by the electron poor  $\text{Tp}^{\text{Ph}_2}$  ligand finding that the dithiocarbamate and in the case of cobalt the  $\text{Tp}^{\text{Ph}_2}$  ligand are bound asymmetrically.<sup>19</sup> We hypothesized that an asymmetrically bound  $\text{Tp}^{\text{Ph}_2}$  and dithiocarbamate ligand should allow us to mimic some features of the azurin active site. In this paper we report the synthesis, structural and electrochemical studies of  $[\text{Tp}^{\text{Ph}_2}\text{Cu}(\text{dte})]$  ( $\text{dte} = \text{S}_2\text{CNEt}_2$  **1**,  $\text{S}_2\text{CNBz}_2$  **2** and  $\text{S}_2\text{CN}(\text{CH}_2)_4$  **3**) and rationalize our results with DFT calculations.

## Results and Discussion

### Synthesis and basic characterization of $[\text{Tp}^{\text{Ph}_2}\text{Cu}(\text{dte})]$

The reaction of  $\text{CuCl}_2 \cdot 2\text{H}_2\text{O}$  with  $\text{KTp}^{\text{Ph}_2}$  yields the intermediate  $[\text{Tp}^{\text{Ph}_2}\text{CuCl}]$  as a green solution. Subsequent addition of  $\text{Na}(\text{dte})$  results in a gradual change in colour to dark green and after work-up the compounds  $[\text{Tp}^{\text{Ph}_2}\text{Cu}(\text{dte})]$  ( $\text{dte} = \text{S}_2\text{CNEt}_2$  **1**,  $\text{S}_2\text{CNBz}_2$  **2** and  $\text{S}_2\text{CN}(\text{CH}_2)_4$  **3**; Scheme 1) are isolated in good yields.  $[\text{Tp}^{\text{Ph}_2}\text{CuCl}(\text{MeOH})]$  was used as an intermediate as the isolated complex from this reaction is  $[\text{Tp}^{\text{Ph}_2}\text{CuCl}(\text{Hpz}^{\text{Ph}_2})]$  formed as a result of decomposition of the  $\text{Tp}^{\text{Ph}_2}$  ligand.<sup>20</sup> This latter complex proved to be less suitable for use as a starting material with lower yields in all cases.



Scheme 1 Synthesis of **1-3**.

IR spectroscopic studies of **1-3** reveal B-H stretches between 2619–2586  $\text{cm}^{-1}$  and consistent with  $\kappa^3$  coordinated  $\text{Tp}^{\text{Ph}_2}$  (Table 1). Similar bands have been observed for other five coordinate  $[\text{Tp}^{\text{Ph}_2}\text{CuL}]$  compounds.<sup>19–22</sup> Examining the dithiocarbamate stretches we find that the C-N stretch is observed at 1478–1503  $\text{cm}^{-1}$  and indicative of a bidentate coordination mode.<sup>23</sup> This is approximately 20  $\text{cm}^{-1}$  higher than the corresponding  $[\text{Tp}^{\text{Ph}_2}\text{M}(\text{dte})]$  ( $\text{M} = \text{Co}, \text{Ni}$ ) complexes.<sup>19</sup> In addition, there is a concomitant decrease in the energy of the C-S stretch this time by 5–10  $\text{cm}^{-1}$ . The changes in the C-N and C-S stretches suggest a greater prevalence of the thiourea resonance form in the case of the copper complexes.

Table 1 Spectroscopic data for  $[\text{Tp}^{\text{Ph}_2}\text{Cu}(\text{dte})]$  **1-3**.

Complex	IR ( $\text{cm}^{-1}$ ) <sup>a</sup>			UV-Vis (nm, $\epsilon$ )
	$\nu_{\text{BH}}$	$\nu_{\text{CN}}$	$\nu_{\text{CS}}$	
<b>1</b>	2619	1478	1008	417 (4,880), 664 (373)
<b>2</b>	2613	1503	997	428 (12,900), 580sh (780)
<b>3</b>	2586	1481	1009	430 (25,200), 620sh (1,650)

<sup>a</sup>As KBr discs

Following ESR spectroscopic studies (*vide infra*) we undertook solution IR spectroscopic studies for **3** in  $\text{CH}_2\text{Cl}_2$ . The solution initially contains a single band at 2593  $\text{cm}^{-1}$  but after 10 minutes a small band is observed at 2522  $\text{cm}^{-1}$  consistent with the  $\text{Tp}^{\text{Ph}_2}$  ligand being  $\kappa^2$  coordinated (see Figure S1).<sup>24</sup> This suggests that in solution, **3** exists as a mixture of  $\kappa^3$  and  $\kappa^2$  species (Figure 1). The low intensity of the peak at 2522  $\text{cm}^{-1}$  indicates that the equilibrium lies towards the five coordinate  $\kappa^3$  complex, a fact confirmed by UV-Vis and ESR spectroscopic studies.

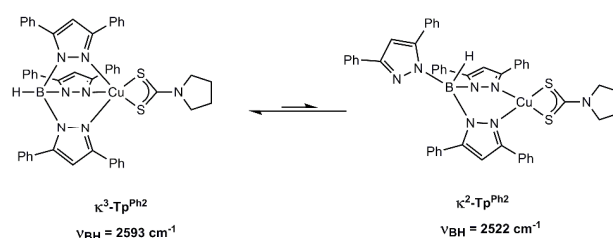


Figure 1  $\kappa^3$  to  $\kappa^2$  isomerisation in  $[\text{Tp}^{\text{Ph}_2}\text{Cu}(\text{S}_2\text{CN}(\text{CH}_2)_4)]$  **3** (values in  $\text{CH}_2\text{Cl}_2$ ).

Although, no identical system exists in  $\text{Cu}(\text{II})$   $\text{Tp}^{\text{R}}$  chemistry  $\kappa^2$ - $\kappa^3$  isomerisation is known in  $[\text{Tp}^{\text{Me}_2}\text{RhL}(\text{CO})]$  ( $\text{Tp}^{\text{Me}_2} =$  hydrotris(3,5-dimethylpyrazolyl)borate,  $\text{L} =$  phosphine) and  $[\text{Tp}^{\text{iPr}_2}\text{Rh}(\text{nbd})]$  ( $\text{nbd} =$  norbornadiene) with the balance between the isomers so fine in the latter case that both isomers crystallize in the same unit cell.<sup>24–26</sup> Moreover, using a modified  $\text{Tp}$  ligand,  $\text{PhB}(3\text{-C}_2\text{F}_2\text{pz})_3$  ( $3\text{-C}_2\text{F}_2\text{pz} = 3\text{-pentafluoroethylpyrazole}$ )  $\kappa^2$ -coordinated  $\text{PhB}(3\text{-C}_2\text{F}_2\text{pz})_3$  is found in the  $\text{Cu}(\text{I})$  complex,  $[\{\text{PhB}(3\text{-C}_2\text{F}_2\text{pz})_3\}\text{Cu}(\eta^2\text{-H}_2\text{C}=\text{CH}_2)]$ .<sup>27</sup>

The UV-Vis spectra were recorded in  $\text{CH}_2\text{Cl}_2$  and are shown in Figure 2. The spectra are dominated by a single intense band at *ca.* 430 nm. By comparison with other five coordinate copper compounds this is assigned to a S ( $p_\pi$ )-to- $\text{Cu}^{2+}$  LMCT band.<sup>9,28,29</sup> In contrast, azurin absorbs at 628 nm making the protein appear blue. The presence of a stronger band at higher energy in **1-3** in solution is due to stronger axial coordination to the  $\text{Cu}^{2+}$  centre (and thus more effective overlap of the  $d_{x^2-y^2}$  orbital with the S  $\sigma$  orbital) rather than the very weak axial bonds found in azurin ( $\text{Cu-S}(\text{met}) = 3.26 \text{ \AA}$  and  $\text{Cu-O}(\text{gly}) = 2.94 \text{ \AA}$ ), which favours overlap with the S  $\pi$  orbital. Indeed, studies on variants of azurin with stronger donor amino acids have shown transformation of the blue copper protein into a green copper protein. However, there are weaker bands found at 580–664 nm which may assigned to a S ( $p_\pi$ )-to- $\text{Cu}^{2+}$  LMCT band.<sup>9,28,29</sup> It is noteworthy that the position and intensity of the band is strongly dependent on the dithiocarbamate ligand increasing in the order **1** < **2** < **3**. A similar shift in the charge

transfer bands is noted in  $[\text{Tp}^{\text{Ph}_2}\text{Ni}(\text{dte})]$ , although for the nickel compounds the intensity of the transition among these compounds is essentially the same. The presence of small amounts of the  $\kappa^2$  complex in the case of **3** may also influence the intensity of this band. Particularly striking is the increase in the intensity of the band at 430 nm compared with  $[\text{Tp}^{\text{Ph}_2}\text{Ni}(\text{dte})]$  by a factor of *ca.* 10.<sup>19</sup> Interestingly, there is also a significant increase in intensity in the S ( $p_\pi$ )-to- $\text{Cu}^{2+}$  LMCT band on moving from Ni to Cu in the  $[\text{Tp}^{\text{i-Pr}_2}\text{M}(\text{SC}_6\text{F}_5)]$  series.<sup>18</sup> There are no obvious features in the spectra above 750 nm consistent with the results reported by Solomon *et al.* for  $[\text{Tp}^{\text{i-Pr}_2}\text{Cu}(\text{SMelM})]$  (SMelM = 1-methylimidazole-2-thiolate).<sup>29</sup>

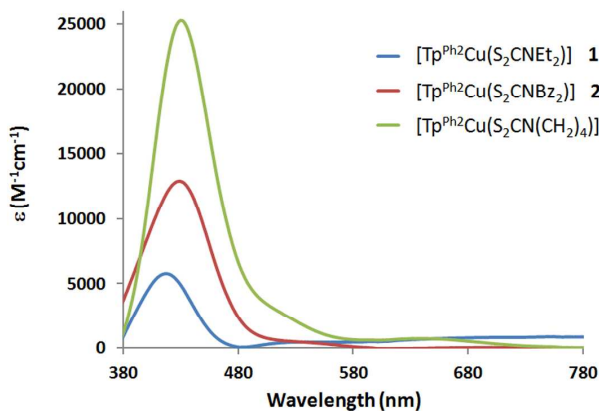


Figure 2 UV-Vis spectra of  $[\text{Tp}^{\text{Ph}_2}\text{Cu}(\text{dte})]$  1-3.

### Structural studies of $[\text{Tp}^{\text{Ph}_2}\text{Cu}(\text{dte})]$

The compounds have been crystallized from  $\text{CH}_2\text{Cl}_2/\text{hexane}$  and their structures determined by X-ray crystallography. Crystallographic data are presented in Tables 2 and 3 while Figure 3 shows the structure of **3** as a representative example (Figures S2 and S3 for **1** and **2**, respectively are contained in the ESI). The structures are all broadly similar with a five coordinate Cu centre. The geometry around the copper centre is subtly different for the complexes with **1** and **3** slightly closer to a square pyramidal geometry while **2** is closer to a trigonal bipyramidal geometry;  $\tau = 0.39, 0.55$  and  $0.39$  for **1**, **2**, and **3**, respectively.<sup>30</sup> In these structures, S1, S2, N3 and N5 define the basal plane while N1 is in the apical position. In the case of  $[\text{Tp}^{\text{Ph}_2}\text{Cu}(\text{S}_2\text{CNBz}_2)]$ , N1, N5 and S2 are in the equatorial positions while N3 and S1 occupy the axial positions with this geometry preferred probably due to the greater steric bulk of the benzyl substituents. Similar distortion parameters have been reported in the related Co and Ni complexes ( $\tau = 0.40$ - $0.46$ ), although none of these structures contains the dibenzylidithiocarbamate ligand.<sup>19</sup> Very recently, the structure of  $[\text{Tp}^{\text{Me}_2}\text{Cu}(\text{S}_2\text{CNET}_2)]$  was reported and also displays a square pyramidal geometry ( $\tau = 0.37$ ) which is similar to **1-3** despite the different  $\text{Tp}^{\text{R}}$  ligands.<sup>31</sup> The only other crystallographically characterized Cu(II)  $\text{Tp}^{\text{R}}$  complex with an  $\text{N}_3\text{S}_2$  donor set is  $[\text{Cu}(\text{Tp}^{\text{Ph}_2-\text{SMe}})]^+$  ( $\text{Tp}^{\text{Ph}_2-\text{SMe}}$  = hydrotris[3-2-(methylsulfanyl)-

phenylpyrazol-1-yl]borate) which also has a square pyramidal geometry ( $\tau = 0.15$ ).<sup>32</sup>

Table 2 Bond lengths and angles for  $[\text{Tp}^{\text{Ph}_2}\text{Cu}(\text{dte})]$  1-3. ( $\text{\AA}$ ,  $^\circ$ ).

	1	2	3
Cu-N1	2.236(3)	2.236(4)	2.235(3)
Cu-N3	2.047(3)	2.024(4)	2.040(3)
Cu-N5	2.038(3)	2.058(4)	2.031(3)
Cu-S1	2.331(1)	2.336(2)	2.340(1)
Cu-S2	2.327(1)	2.312(2)	2.321(1)
S1-Cu-S2	75.65(4)	75.97(5)	76.13(3)
N1-Cu-S1	97.37(8)	96.2(1)	111.88(7)
N1-Cu-S2	113.95(8)	123.3(1)	95.55(7)
N3-Cu-S1	174.89(8)	175.2(1)	152.86(8)
N3-Cu-S2	101.18(8)	99.2(1)	96.56(8)
N5-Cu-S1	95.56(8)	95.7(1)	100.76(8)
N5-Cu-S2	151.46(8)	142.0(1)	176.39(8)
N1-Cu-N3	87.6(1)	86.7(2)	94.7(1)
N1-Cu-N5	93.9(1)	94.2(2)	87.3(1)
N3-Cu-N5	85.4(1)	87.9(2)	85.4(1)

In contrast to  $[\text{Tp}^{\text{Ph}_2}\text{M}(\text{dte})]$  ( $\text{M} = \text{Co}, \text{Ni}$ ), one of the Cu-N bond lengths is *ca.*  $0.2 \text{ \AA}$  longer than the other two indicating that the  $\text{Tp}^{\text{Ph}_2}$  ligand is asymmetrically coordinated.<sup>19</sup> Similar observations have been made concerning other five coordinate  $[\text{Tp}^{\text{R}}\text{Cu}(\text{L})]$  complexes and are consistent with complete occupation of the  $d_{z^2}$  orbital.<sup>20,21,29</sup> The Cu-S bond lengths are *ca.*  $0.07 \text{ \AA}$  shorter on average than the Ni compounds and consistent with the different ionic radii of Ni(II) and Cu(II). Moreover, the Cu-S bond lengths are more typical of a type 2 Cu centre (Cu-Cys  $2.29 \text{ \AA}$ ).<sup>1</sup> Surprisingly, the dithiocarbamate ligands are essentially symmetrically bound in all complexes while in the analogous Co and Ni systems the ligands are asymmetrically bound.<sup>19</sup>

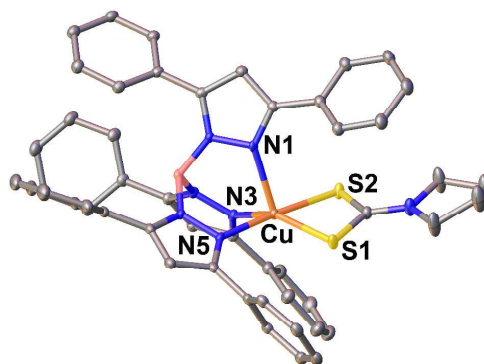


Figure 3 Structure of  $[\text{Tp}^{\text{Ph}_2}\text{Cu}(\text{S}_2\text{CN}(\text{CH}_2)_4)]$  **3**. Hydrogen atoms are omitted and only selected atoms labelled in the interests of clarity.

In addition, the S-Cu-S bite angles are  $75.7, 76.0$  and  $76.5^\circ$  and slightly larger than those found in  $[\text{Tp}^{\text{Ph}_2}\text{M}(\text{dte})]$  ( $\text{M} = \text{Co}, \text{Ni}$ ) consistent with the shorter M-S bond lengths in the Cu(II) compounds. Overall, as planned one of the pyrazolyl donors of the  $\text{Tp}^{\text{Ph}_2}$  ligand is coordinated loosely to the Cu centre mimicking the weakly coordinated glycine residue in azurin. Sadly, the dithiocarbamate ligand does not coordinate

asymmetrically and thus the coordination environment more closely resembles so-called green copper proteins than azurin.

**Table 3** Crystallographic data and structure refinement parameters for **1-3**.

	1	2	3
Formula	C <sub>50</sub> H <sub>44</sub> BCuN <sub>7</sub> S <sub>2</sub>	C <sub>60</sub> H <sub>48</sub> BCuN <sub>7</sub> S <sub>2</sub>	C <sub>50</sub> H <sub>42</sub> BCuN <sub>7</sub> S <sub>2</sub>
Molecular weight / g mol <sup>-1</sup>	881.39	1005.52	879.38
Crystal system	Monoclinic	Monoclinic	Monoclinic
Space group	P2 <sub>1</sub> /c	P2 <sub>1</sub> /c	P2 <sub>1</sub> /c
a / Å	13.9619(7)	17.804(5)	13.9204(14)
b / Å	25.3276(14)	18.099(5)	25.042(3)
c / Å	12.5670(6)	17.810(5)	12.6285(13)
α / °	90	90	90
β / °	104.037(3)	119.686(6)	102.523(2)
γ / °	90	90	90
T / K	100(2)	150(2)	100(2)
Cell volume / Å <sup>3</sup>	4311.3(4)	4986(2)	4297.4(8)
Z	4	4	4
Absorption coefficient / mm <sup>-1</sup>	0.649	0.570	0.651
Reflections collected	40791	41115	25061
Independent reflections, R <sub>int</sub>	9752, 0.0899	11407, 0.1298	8000, 0.0655
Max. and min. transmission	0.9808 and 0.7953	0.9452 and 0.8297	0.8809 and 0.7368
Restraints/parameters	0/552	507/640	416/550
Final R indices [I > 2σ(I)]: R <sub>1</sub> , wR <sub>2</sub>	0.0601, 0.1773	0.0689, 0.2489	0.0448, 0.1717

### ESR spectroscopic studies of [Tp<sup>Ph2</sup>Cu(dtc)]

ESR spectra of **1-3** were recorded in CH<sub>2</sub>Cl<sub>2</sub> at 295 K and also in frozen CH<sub>2</sub>Cl<sub>2</sub> at 150 K. The isotropic spectra are shown in Figure 4 with anisotropic spectra in the supporting information (Figure S4). ESR parameters at 295 and 150 K in solution and as a glass are given in Table 4. The spectra of **1-3** display four well resolved lines consistent with hyperfine coupling to <sup>63</sup>Cu and <sup>65</sup>Cu (I = 3/2).<sup>20,21</sup> There is also hyperfine coupling to the N atoms of the Tp<sup>Ph2</sup> ligand on the m<sub>l</sub> = -3/2 line. Similar observations have been made concerning a range of five coordinate [Tp<sup>R</sup>CuX(Hpz<sup>R</sup>)] (X = Cl, OAc) complexes and [Tp<sup>ipr2</sup>Cu-(SMelm)] suggesting that the structure found in the crystallographic studies is preserved in solution.<sup>20,21,29</sup> It should be noted that the spectrum of **3** contains an additional species at higher field consistent with the four coordinate κ<sup>2</sup> species observed in the IR spectroscopic studies. Moreover, integration of the spectra clearly indicate that there are only 2 species in solution in **3** and a single species for **1** and **2** (Figure S5). We have also explored the effect of time on the spectrum of **3** and find that the equilibrium is rapid being reached after 10 minutes and then remaining unchanged even after 4 hours (Figure S7). However, changing the concentration does result in a change in the spectrum further supporting the proposed κ<sup>3</sup> to κ<sup>2</sup> isomerisation (Figure S8). We hypothesize that as the concentration increases the individual molecules become closer allowing formation of favourable interactions but only if the Tp<sup>Ph2</sup> ligand becomes κ<sup>2</sup>-coordinated.

**Table 4** ESR parameters for **1-3** at 295 and 150 K.

	g	A <sup>63,65</sup> Cu x 10 <sup>4</sup> (cm <sup>-1</sup> )	A <sup>14</sup> N x 10 <sup>4</sup> (cm <sup>-1</sup> )
<b>1</b>	2.085 (g <sub>iso</sub> )	70	7
	2.18 (g <sub>  </sub> )	145 (A <sub>  </sub> )	-
	2.03 (g <sub>⊥</sub> )	-	-
<b>2</b>	2.086 (g <sub>iso</sub> )	70	7
	2.18 (g <sub>  </sub> )	140 (A <sub>  </sub> )	-
	2.03 (g <sub>⊥</sub> )	-	-
<b>3<sup>a</sup></b>	2.085 (g <sub>iso</sub> )	73	7
	2.19 (g <sub>  </sub> )	150 (A <sub>  </sub> )	-
	2.03 (g <sub>⊥</sub> )	-	-

<sup>a</sup> Simulated ESR spectra at 295 K may be found in the ESI (Figure S6)

While an exactly similar system is not known in Cu(II) Tp<sup>R</sup> chemistry, [Cu(Br<sup>Mes</sup>pz<sup>o-py</sup>)<sub>2</sub>] (hydro[bis(4-mesityl-3-methylthioxotriazolyl)-3-(2-pyridyl)pyrazolyl]borate) exists as a S<sub>2</sub>N<sub>2</sub> bonded dimer in the solid state with two thioxotriazolyl donors from one ligand and a pyrazolyl and pyridyl donor from another Br<sup>Mes</sup>pz<sup>o-py</sup> ligand.<sup>33</sup> In solution this dimer is fluxional with an equilibrium between the S<sub>2</sub>N<sub>2</sub> and S<sub>2</sub>N Cu coordinated dimers in which the pyridyl ligand in the latter dimer is now non-bonded to the Cu centre. It follows that a similar situation may occur in **3**.

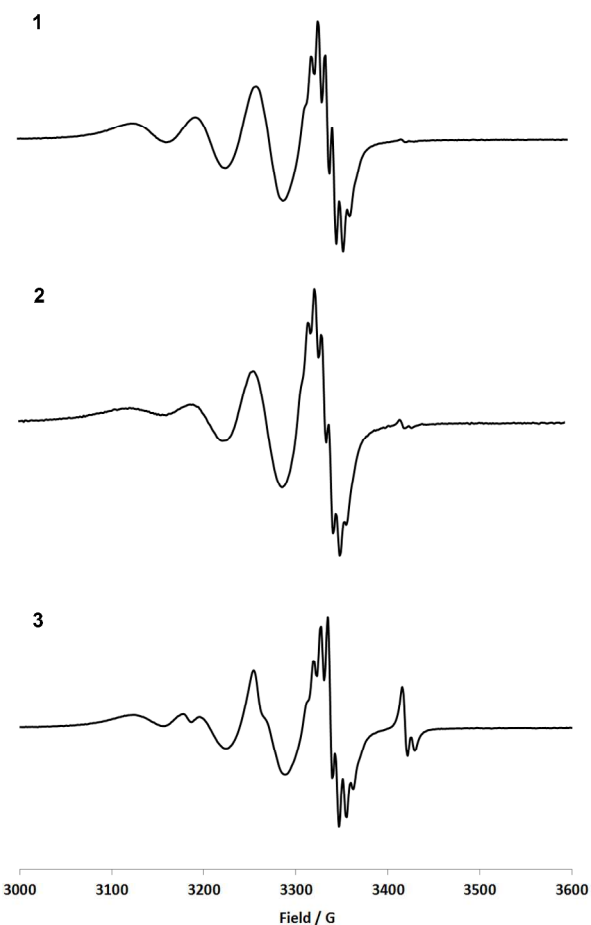


**Figure 4** ESR spectra of **1, 2** and **3** in CH<sub>2</sub>Cl<sub>2</sub> at 295 K.

The spectra are similar to those previously reported for [Cu(dtc)<sub>2</sub>]<sup>34</sup> and [Cu(dtc)(S<sub>2</sub>P(i-Pr)<sub>2</sub>)]<sup>35</sup> and suggest that the

SOMO is likely to be Cu and dithiocarbamate based, a fact later confirmed by DFT calculations.

The ESR spectra of the samples at 150 K in  $\text{CH}_2\text{Cl}_2$  reveal pseudo-axial symmetry and are characteristic of a tetragonal  $\{d_{x^2-y^2}\}^1$  electronic structure in line with the structural studies above. Although the  $g$  values for **1-3** are broadly similar to azurin ( $g_z = 2.262$ ,  $g_y = 2.056$ ,  $g_x = 2.042$ ), the hyperfine coupling to  $^{63,65}\text{Cu}$  in **1-3** varies from 140-150 G and is typical of 'normal' Cu(II) and very much larger than that of azurin ( $A_z = 59$  G) consistent with the stronger Cu-S bonds found in **1-3**. It is also important to note that the spectra are now virtually identical and clearly indicate that the higher field species in the room temperature spectrum of **3** is converted to a single five coordinate species at 150 K consistent with the proposed  $\kappa^3$  to  $\kappa^2$  isomerisation of the  $\text{Tp}^{\text{Ph}_2}$  ligand and ruling out any possible impurity in the sample.

### Electrochemical studies of $[\text{Tp}^{\text{Ph}_2}\text{Cu}(\text{dtc})]$

The native azurin copper enzyme has a reversible well defined  $\text{Cu}^{\text{III/I}}$  redox couple at ca. 0.27 V (NHE).<sup>1</sup> In view of this we investigated the redox properties of these model complexes in  $\text{CH}_2\text{Cl}_2$  using cyclic voltammetry. Representative cyclic voltammograms are shown in Figure 5 with data for the compounds given in Table 5. All the compounds exhibit a reversible one-electron oxidation which is tentatively assigned to oxidation of the coordinated dithiocarbamate ligand oxidation of the coordinated dithiocarbamates based on computational studies (*vide infra*). For **1-3** the redox couple is observed between 0.76-0.80 V and is consistent with the relatively minor alterations in the dithiocarbamates in this series. Compared with  $[\text{Cu}(\text{S}_2\text{CNET}_2)_2]$ , **1** is found to be 0.65 V harder to oxidize consistent with the presence of the more electron poor  $\text{Tp}^{\text{Ph}_2}$  ligand.<sup>36</sup>

Interestingly, the CVs of **1** and **3** include a small peak at ca. 0.50 V which based on the IR and ESR spectroscopic studies is assigned to the  $\kappa^2$  coordinated isomer. The fact that this is absent in **2** clearly indicates that the  $\kappa^3$  to  $\kappa^2$  isomerisation is very sensitive to the electronic properties of the R groups on the dithiocarbamate as would be expected in such an isomerisation process. The presence of a significant peak at 0.50 V in the case of **1** is unexpected as ESR and UV-Vis spectroscopic studies both suggest that there is very little of the  $\kappa^2$  species. This apparent inconsistency is probably due to the electrolyte used in the electrochemical studies. As Gieger and co-workers have shown electrolytes can affect the position of the redox potentials and in our system it's not unreasonable to suppose that it may affect the relative stability of the two isomers in **1**.<sup>37</sup>

**Table 5** Electrochemical data for **1-3**.

	Oxidation ( $E_{1/2}$ , V)	$\text{Cu}^{2+} / \text{Cu}^+$ (V)
<b>1</b>	0.77	-1.02(I) <sup>a</sup>
<b>2</b>	0.80	-1.01(I) <sup>a</sup>
<b>3</b>	0.76	-0.90(I)

<sup>a</sup> (I) = Irreversible.

A reduction peak is observed for all compounds between 0.90-1.02 V. By comparison with  $[\text{Cu}(\text{S}_2\text{CNET}_2)_2]$ , where reduction occurs at -0.86 V, this peak is assigned to reduction to Cu(I). The peak is much lower than that observed for azurin and reflects the strongly electron donating character of the dithiocarbamate ligand and the five coordinate Cu centre in **1-3** compared with the more trigonal planar environment found in azurin.

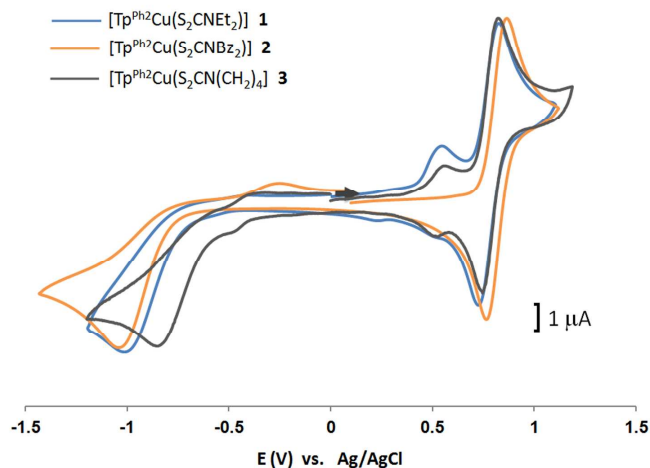


**Figure 5** Cyclic voltammograms of **1-3** in  $\text{CH}_2\text{Cl}_2$  at 100 mV/s.

### DFT calculations of $[\text{Tp}^{\text{Ph}_2}\text{Cu}(\text{dtc})]$

DFT calculations were performed on all the complexes to try to better understand the electronic structure of **1-3**. All calculations were performed using the Gaussian 03 software package<sup>38</sup> with the B3LYP functional and a 6-31G\*\* or SDD basis set. Computed bond lengths and those found in the X-ray crystal structure are shown in Table 6. Comparing the SDD and 6-31G\*\* basis sets we find that the latter is better with a mean standard deviation of 0.066 and 0.041 Å, respectively and thus the following discussion will focus on the 6-31G\*\* basis set. The axial Cu-N distances differs from that found experimentally by between 0.069 – 0.097 Å. Similar discrepancies have been noted in modelling the related four coordinate  $[\text{Tp}^{\text{i-Pr}_2}\text{Cu}(\text{SC}_6\text{F}_5)]$  complexes and simply reflect the weakness of this Cu-N interaction and the comparatively small energy difference between structures even when the Cu-N bond length increases by 0.1 Å.<sup>18</sup> Interestingly, the Cu-S bond lengths are overestimated by as much as 0.08 Å but are consistent with the deviations reported in the analogous Co and Ni complexes,  $[\text{Tp}^{\text{Ph}_2}\text{M}(\text{dtc})]$ .<sup>19</sup> Moreover, the dithiocarbamate ligands are computed to coordinate symmetrically just as is found in the crystal structures. Overall, the DFT calculations adequately model the complexes.

The SOMO for each complex is essentially identical, with **1** shown in Figure 6 as a representative example. The SOMO is found to be a weakly antibonding Cu  $d\pi^*$ -S interaction constructed from an asymmetric combination of the S  $p_z$  orbitals and a Cu  $d_{xz}$  orbital. The metal only contributes ca. 10

% to this orbital with electron density mostly present on the S atoms. Interestingly, a similar Cu-S  $\pi^*$  interaction is found in azurin also with significant delocalization of electron density onto the cysteine residue.<sup>39</sup>

**Table 6** Computed and X-ray crystallographically determined bond lengths for  $[\text{Tp}^{\text{Ph}_2}\text{Cu}(\text{dtc})]$  (Å).

	1 <sup>a</sup>	2 <sup>a</sup>	3 <sup>a</sup>
Cu-N1	2.236(3) 2.139	2.236(4) 2.159	2.235(3) 2.166
Cu-N3	2.047(3) 2.047	2.024(4) 2.046	2.040(3) 2.047
Cu-N5	2.038(3) 2.072	2.058(4) 2.059	2.031(3) 2.050
Cu-S1	2.331(1) 2.397	2.336(2) 2.399	2.340(1) 2.404
Cu-S2	2.327(1) 2.399	2.312(2) 2.394	2.321(1) 2.400

<sup>a</sup> Computed values using a B3LYP functional and a 6-31G\* basis set are shown beneath the experimentally observed values.

For **1-3**, this delocalization may explain why the dithiocarbamate is found to influence the electrochemical behaviour and in particular the presence of peaks due to the  $\kappa^3$  and  $\kappa^2$  species in **1** and **3**. In contrast, in the related Co and Ni complexes the SOMO is a strong antibonding M-S  $\sigma^*$  bond. However, this is consistent with the findings of Fujisawa *et al.* for  $[\text{Tp}^{\text{iPr}_2}\text{M}(\text{SC}_6\text{F}_5)]$  where there is an increasing  $\pi$  contribution on going from Mn(II) to Cu(II).<sup>18</sup>

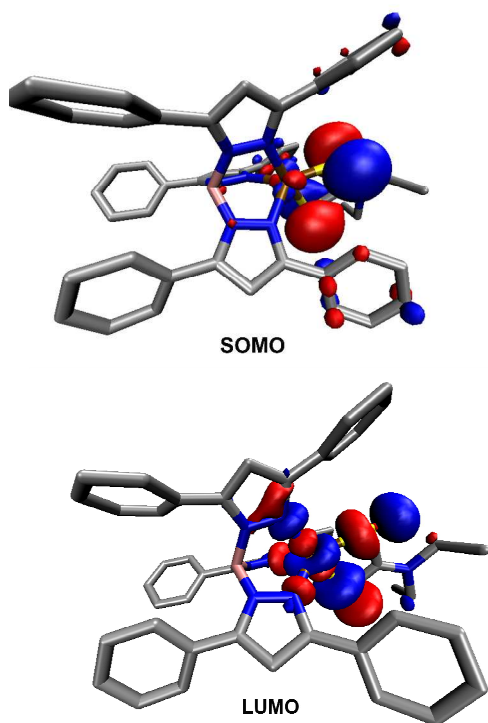


**Figure 6** SOMO and LUMO of  $[\text{Tp}^{\text{Ph}_2}\text{Cu}(\text{S}_2\text{CNEt}_2)]$ .

The two orbitals below the SOMO also contain significant M-S interactions with the SOMO-1 containing a Cu-S  $\pi^*$  interaction, this time involving a symmetric combination of the

S  $p_z$  orbitals and a Cu  $d_{yz}$  orbital. In contrast, the SOMO-2 is weakly antibonding and comprises a Cu-S  $\sigma^*$  bond. Interestingly, a similar order of  $\pi$ - and  $\sigma$  bonds is found in  $[\text{Tp}^{\text{iPr}_2}\text{Cu}(\text{SC}_6\text{F}_5)]$  despite this compound being four coordinate.<sup>18</sup> Finally, the LUMO in all the complexes is a strongly antibonding Cu-S  $\sigma^*$  orbital being an asymmetric combination of a S  $p_x$  and  $p_y$  orbital and a Cu  $d_{x^2-y^2}$  orbital (see Figure 6). This orbital is strongly Cu based (*ca.* 60%) and supports our assignment of the reduction process observed in the CV as being due to Cu(I).

## Conclusions

In conclusion, we have successfully prepared a series of copper dithiocarbamate complexes. The tris(pyrazolyl)borate ligand proves to be a very suitable supporting ligand allowing isolation of mixed ligand complexes with an  $\text{N}_3\text{S}_2$  donor set. Structural studies have revealed that as expected the  $\text{Tp}^{\text{Ph}_2}$  ligand is asymmetrically coordinated with a single elongated Cu-N bond while the dithiocarbamate is symmetrically coordinated giving compounds which more closely resemble copper green proteins. Spectroscopic studies indicate that the compounds are mostly five coordinate in solution, although a  $\kappa^3$  to  $\kappa^2$  isomerisation of the  $\text{Tp}^{\text{Ph}_2}$  ligand exists in the case of **3** and to a lesser extent in **1**. Electrochemical studies are consistent with the spectroscopic findings and reveal only minor changes in the positions of the redox potentials but emphasize the effect that even subtle changes in the R groups on the dithiocarbamate ligand can have a significant impact on the relative stability of the  $\kappa^2$  and  $\kappa^3$  isomers. Overall, these studies highlight the difficulties in successfully modelling a *nominally* five coordinate enzyme like azurin where one of the sulfur donors is so loosely bound. However, they do provide a new model for green copper proteins. Future work will focus on developing asymmetric S,S donor ligands which may be used with the hope of more accurately modelling the azurin active site.

## Experimental Section

### General Remarks

All manipulations were performed in air with HPLC grade solvents. Tris(3,5-diphenylpyrazolyl)borate ( $\text{KTp}^{\text{Ph}_2}$ ) was prepared by a literature procedure.<sup>40</sup> All other chemicals were purchased from Fluka or Aldrich Chemical Company and used as received.

Infrared spectra (as KBr discs) were recorded on a Perkin-Elmer Spectrum One infrared spectrophotometer in the range 400-4000  $\text{cm}^{-1}$ . Electronic spectra were recorded in  $\text{CH}_2\text{Cl}_2$  at room temperature on a Shimadzu UV-1700 UV-Visible spectrophotometer. ESR spectra were recorded at 295 K on a Bruker Biospin ELEXSYS-II E500 spectrometer using a silica flat cell for  $\text{CH}_2\text{Cl}_2$  solutions and a 3 mm diameter cylindrical silica cell for solid samples. The ESR modulation amplitude = 0.1 G, time constant = 10 ms and microwave power = 0.2 mW. Elemental analyses were carried out on a Eurovector EA3000

analyser. ESI-MS were carried out on a Bruker Daltonics 7.0T Apex 4 FTICR Mass Spectrometer. Electrochemical studies were carried out using a palmsensPC Vs 2.11 potentiostat in conjunction with a three electrode cell. The auxiliary electrode was a platinum rod and the working electrode was a platinum disc (2.0 mm diameter). The reference electrode was a Ag-AgCl electrode. Solutions in CH<sub>2</sub>Cl<sub>2</sub> dried over CaH<sub>2</sub>, were 5 × 10<sup>-4</sup> mol·dm<sup>-3</sup> in the test compound and 0.1 mol·dm<sup>-3</sup> in [NBu<sup>n</sup>][PF<sub>6</sub>] as the supporting electrolyte. Under these conditions, E<sup>o</sup> for the one-electron oxidation of [Fe(η-C<sub>5</sub>Me<sub>5</sub>)<sub>2</sub>] added to the test solutions as an internal calibrant is -0.08 V.

### Synthesis of complexes

#### [Tp<sup>Ph2</sup>Cu(S<sub>2</sub>CNET<sub>2</sub>)<sub>2</sub>] 1

CuCl<sub>2</sub>·2H<sub>2</sub>O (85 mg, 0.5 mmol) was dissolved in MeOH (10 ml) giving a green solution. KTp<sup>Ph2</sup> (354 mg, 0.5 mmol) was dissolved in THF (5 ml) and added to the solution resulting in a red-brown solution which was stirred for 1 hr. NaS<sub>2</sub>CNET<sub>2</sub> (113 mg, 0.55 mmol) was then added resulting in a gradual change to dark green. The solution was stirred for 3 hrs and reduced to dryness *in vacuo*. The solid was redissolved in CH<sub>2</sub>Cl<sub>2</sub> (2 ml), filtered and layered with hexanes (15 ml). After 2 days dark green crystals formed which were washed with Et<sub>2</sub>O (2 × 5 ml) and air dried (303 mg, 69%). ν<sub>max</sub>(KBr)/cm<sup>-1</sup> 3055, 2973, 2931 (ν<sub>CH</sub>), 2619 (ν<sub>BH</sub>), 1478 (ν<sub>C=N</sub>), 1008 (ν<sub>CS</sub>). UV-Vis λ<sub>max</sub>(CH<sub>2</sub>Cl<sub>2</sub>)/nm (ε, dm<sup>3</sup>mol<sup>-1</sup>cm<sup>-1</sup>) 417 (4,880), 664 (373). *m/z* (ESI) 732 [M-S<sub>2</sub>CNET<sub>2</sub>]<sup>+</sup>. Anal. Calc. for C<sub>50</sub>H<sub>44</sub>N<sub>7</sub>BS<sub>2</sub>Cu: C 68.49, H 5.06, N 11.18; Found: C 68.35, H 5.02, N 11.13.

Complexes **2-3** were synthesized in a similar manner to **1** using the appropriate dithiocarbamate salt and recrystallized from the solvents indicated.

#### [Tp<sup>Ph2</sup>Cu(S<sub>2</sub>CNBZ<sub>2</sub>)<sub>2</sub>] 2

Dark green crystals (crystallised from CH<sub>2</sub>Cl<sub>2</sub>-hexane). 58% yield. ν<sub>max</sub>(KBr)/cm<sup>-1</sup> 3056, 3027, 2937 (ν<sub>CH</sub>), 2613 (ν<sub>BH</sub>), 1503 (ν<sub>C=N</sub>), 997 (ν<sub>CS</sub>). UV-Vis λ<sub>max</sub>(CH<sub>2</sub>Cl<sub>2</sub>)/nm (ε, dm<sup>3</sup>mol<sup>-1</sup>cm<sup>-1</sup>) 428 (12,900), 580sh (780). *m/z* (ESI) 732 [M-S<sub>2</sub>CNBZ<sub>2</sub>]<sup>+</sup>. Anal. Calc. for C<sub>60</sub>H<sub>48</sub>N<sub>7</sub>BS<sub>2</sub>Cu: C 72.00, H 4.83, N 9.80; Found: C 71.67, H 4.84, N 9.79.

#### [Tp<sup>Ph2</sup>Cu(S<sub>2</sub>CN(CH<sub>2</sub>)<sub>4</sub>)<sub>2</sub>] 3

Dark green crystals (crystallised from CH<sub>2</sub>Cl<sub>2</sub>-hexane). 55% yield. ν<sub>max</sub>(KBr)/cm<sup>-1</sup> 3058, 2970 (ν<sub>CH</sub>), 2586 (ν<sub>BH</sub>), 1481 (ν<sub>C=N</sub>), 1009 (ν<sub>CS</sub>). UV-Vis λ<sub>max</sub>(CH<sub>2</sub>Cl<sub>2</sub>)/nm (ε, dm<sup>3</sup>mol<sup>-1</sup>cm<sup>-1</sup>) 430 (25,200), 620sh (1,650). *m/z* (ESI) 732 [M-S<sub>2</sub>CN(CH<sub>2</sub>)<sub>4</sub>]<sup>+</sup>. Anal. Calc. for C<sub>50</sub>H<sub>42</sub>N<sub>7</sub>BS<sub>2</sub>Cu: C 68.65, H 4.84, N 11.21; Found: C 68.84, H 5.01, N 11.19.

### X-ray crystallography

Crystal data and data processing parameters for the structures of **1**, **2** and **3** are given in Tables 2 and 3. X-ray quality crystals of **1**, **2** and **3** were grown by allowing hexane to diffuse into a concentrated solution of the complex in CH<sub>2</sub>Cl<sub>2</sub>. Crystals were mounted on a glass fibre using perfluoropolyether oil and cooled rapidly to 100 or 150 K in a stream of cold nitrogen. All

diffraction data were collected on a Bruker Smart CCD area detector with graphite monochromated Mo Kα(λ = 0.71073 Å).<sup>41</sup> After data collection, in each case an empirical absorption correction (SADABS)<sup>42</sup> was applied, and the structures were then solved by direct methods and refined on all *F*<sup>2</sup> data using the SHELX suite of programs.<sup>43</sup> In all cases non-hydrogen atoms were refined with anisotropic thermal parameters; hydrogen atoms were included in calculated positions and refined with isotropic thermal parameters which were *ca.* 1.2 × (aromatic CH, CH<sub>2</sub>) or 1.5 × (Me) the equivalent isotropic thermal parameters of their parent carbon atoms. All pictures were drawn using OLEX2.<sup>44</sup>

### Computational details

All calculations were performed with Gaussian 03 (Revision C.02) and used the B3LYP density functional.<sup>38</sup> The structural properties of the complexes obtained from X-ray crystallographic data were used as initial structures for full optimization. Calculations were performed at the DFT-B3LYP level of theory using a SDD or 6-31G\*\* basis set. Geometry optimizations were performed in the gas phase for each given spin state. The molecular orbital analyses were then conducted at those geometries. The SOMO and LUMO three-dimensional isosurface plots were generated using Avogadro.<sup>45</sup>

### Acknowledgements

We gratefully acknowledge the Thailand Research Fund (Grant No. RMU5080029 and RSA5580028) for funding this work. The Development and Promotion of Science and Technology Talents Project is thanked for a scholarship to WP.

### Notes and references

- <sup>a</sup> Molecular Technology Research Unit Cell, Walailak University, Thasala, Nakhon Si Thammarat, 80161, Thailand, Fax: (+66) 75-672004 E-mail: hdavid@wu.ac.th.
  - <sup>b</sup> Department of Chemistry, Faculty of Science and Technology, Thammasat University, 99 Paholyothin Rd., Khlong 1, Khlong Luang, Pathum Thani, 12120, Thailand.
  - <sup>c</sup> Division of Chemistry and Biological Chemistry, School of Physical and Mathematical Sciences, Nanyang Technological University, Singapore 637371.
  - <sup>d</sup> Department of Chemistry, University of Sheffield, Sheffield, S3 7HF, United Kingdom.
- Electronic Supplementary Information (ESI) available: ESR spectra at 150 K and varying concentrations and times for **3**, and atomic coordinates for all calculated structures can be found in the ESI. CCDC 940585, 940586 and 940587 contain the supplementary crystallographic data for **1**, **2** and **3**, respectively. These data can be obtained free of charge from The Cambridge Crystallographic Data Centre via [www.ccdc.cam.ac.uk/data\\_request/cif](http://www.ccdc.cam.ac.uk/data_request/cif). See DOI: 10.1039/b000000x/
- E. I. Solomon, R. K. Szilagyi, S. DeBeer George, and L. Basumallick, *Chem. Rev.*, 2004, **104**, 419–58.
  - E. I. Solomon, *Chem. Rev.*, 1992, **92**, 521–542.
  - H. B. Gray, B. G. Malmström, and R. J. P. Williams, *J. Biol. Inorg. Chem.*, 2000, **5**, 551–559.
  - C. Dennison, *Coord. Chem. Rev.*, 2005, **249**, 3025–3054.

5. J. M. Guss, H. D. Bartunik, and H. C. Freeman, *Acta Crystallogr. Sect. B Struct. Sci.*, 1992, **48**, 790–811.
6. K. Paraskevopoulos, M. Sundararajan, R. Surendran, M. a Hough, R. R. Eady, I. H. Hillier, and S. S. Hasnain, *Dalton Trans.*, 2006, 3067–76.
7. E. W. Ainscough, A. G. Bingham, A. M. Brodie, W. R. Ellis, H. B. Gray, T. M. Loehr, J. E. Plowman, G. E. Norris, and E. N. Baker, *Biochemistry*, 1987, **26**, 71–82.
8. E. N. Baker, *J. Mol. Biol.*, 1988, **203**, 1071–1095.
9. K. M. Clark, Y. Yu, N. M. Marshall, N. a Sieracki, M. J. Nilges, N. J. Blackburn, W. a van der Donk, and Y. Lu, *J. Am. Chem. Soc.*, 2010, **132**, 10093–101.
10. T. D. Wilson, M. G. Savelie, M. J. Nilges, N. M. Marshall, and Y. Lu, *J. Am. Chem. Soc.*, 2011, **133**, 20778–20792.
11. A. Chowdhury, L. A. Peteanu, M. A. Webb, and G. R. Loppnow, *J. Phys. Chem. B*, 2001, **105**, 527–534.
12. E. I. Solomon and R. G. Hadt, *Coord. Chem. Rev.*, 2011, **255**, 774–789.
13. M. Roger, F. Biaso, C. J. Castelle, M. Bauzan, F. Chaspoul, E. Lojou, G. Sciara, S. Caffarri, M.-T. Giudici-Ortoni, and M. Ilbert, *PLoS One*, 2014, **9**, e98941.
14. S. Ghosh, X. Xie, A. Dey, Y. Sun, C. P. Scholes, and E. I. Solomon, *Proc. Natl. Acad. Sci. U.S.A.*, 2009, **106**, 4969–4974.
15. I. M. Wasser, S. De Vries, P. Moe, I. Schro, and K. D. Karlin, *Chem. Rev.*, 2002, **102**, 1201–1234.
16. N. Kitajima, K. Fujisawa, and Y. Morooka, *J. Am. Chem. Soc.*, 1990, **112**, 3210–3212.
17. N. Kitajima, K. Fujisawa, M. Tanaka, and Y. Morooka, *J. Am. Chem. Soc.*, 1992, **114**, 9232–9233.
18. S. I. Gorelsky, L. Basumallick, J. Vura-Weis, R. Sarangi, K. O. Hodgson, B. Hedman, K. Fujisawa, and E. I. Solomon, *Inorg. Chem.*, 2005, **44**, 4947–4960.
19. D. J. Harding, P. Harding, S. Dokmaisorijan, and H. Adams, *Dalton Trans.*, 2011, **40**, 1313–21.
20. L. M. L. Chia, S. Radojevic, I. J. Scowen, M. McPartlin, and M. A. Halcrow, *J. Chem. Soc., Dalton Trans.*, 2000, 133–140.
21. C. L. Foster, X. Liu, C. A. Kilner, M. Thornton-Pett, and M. A. Halcrow, *J. Chem. Soc., Dalton Trans.*, 2000, 4563–4568.
22. M. A. Halcrow, J. E. Davies, and P. R. Raithby, *Polyhedron*, 1997, **16**, 1535–1541.
23. K. Nakamoto, *Infrared and Raman Spectra of Inorganic and Coordination Compounds: Part B*, New York, 6th Ed., 2009.
24. M. Akita, K. Ohta, Y. Takahashi, S. Hikichi, and Y. Moro-oka, *Organometallics*, 1997, **16**, 4121–4128.
25. N. G. Connelly, D. J. H. Emslie, W. E. Geiger, O. D. Hayward, E. B. Linehan, A. G. Orpen, M. J. Quayle, and P. H. Rieger, *J. Chem. Soc., Dalton Trans.*, 2001, 670–683.
26. W. E. Geiger, N. C. Ohrenberg, B. Yeomans, N. G. Connelly, and D. J. H. Emslie, *J. Am. Chem. Soc.*, 2003, **125**, 8680–8688.
27. H. V. R. Dias and J. Wu, *Organometallics*, 2012, **31**, 1511–1517.
28. E. I. Solomon, *Inorg. Chem.*, 2006, **45**, 8012–25.
29. L. Basumallick, S. DeBeer, D. W. Randall, B. Hedman, K. O. Hodgson, K. Fujisawa, and E. I. Solomon, *Inorg. Chim. Acta*, 2002, **337**, 357–365.
30. A. W. Addison, T. N. Rao, J. Reedijk, J. van Rijn, and G. C. Verschoor, *J. Chem. Soc., Dalton Trans.*, 1984, 1349.
31. L. M. C. Cañada, G. P. A. Yap, and P. J. Y. Lim, *Acta Crystallogr. Sect. C Cryst. Struct. Commun.*, 2013, **69**, 4–7.
32. E. R. Humphrey, K. L. V Mann, Z. R. Reeves, A. Behrendt, J. C. Jeffrey, J. P. Maher, J. A. McCleverty, and M. D. Ward, *New J. Chem.*, 1999, **23**, 417–423.
33. R. Cammi, M. Gennari, M. Giannetto, M. Lanfranchi, L. Marchio, G. Mori, C. Paiola, and M. A. Pellinghelli, *Inorg. Chem.*, 2005, **44**, 4333–4345.
34. G. Hogarth, *Prog. Inorg. Chem.*, 2005, **53**, 1978–2003.
35. B. G. Jeliaskova and G. C. Sarova, *Polyhedron*, 1997, **16**, 3967–3975.
36. N. G. Berry, T. W. Shimell, and P. D. Beer, *J. Supramol. Chem.*, 2003, **2**, 89–92.
37. F. Barrière and W. E. Geiger, *J. Am. Chem. Soc.*, 2006, **128**, 3980–9.
38. M. J. Frisch, G. W. Trucks, H. B. Schlegel, G. E. Scuseria, M. A. Robb, J. R. Cheeseman, J. A. Montgomery, Jr., T. Vreven, K. N. Kudin, J. C. Burant, J. M. Millam, S. S. Iyengar, J. Tomasi, V. Barone, B. Mennucci, M. Cossi, G. Scalmani, N. Rega, G. A. Petersson, H. Nakatsuji, M. Hada, M. Ehara, K. Toyota, R. Fukuda, J. Hasegawa, M. Ishida, T. Nakajima, Y. Honda, O. Kitao, H. Nakai, M. Klene, X. Li, J. E. Knox, H. P. Hratchian, J. B. Cross, V. Bakken, C. Adamo, J. Jaramillo, R. Gomperts, R. E. Stratmann, O. Yazyev, A. J. Austin, R. Cammi, C. Pomelli, J. W. Ochterski, P. Y. Ayala, K. Morokuma, G. A. Voth, P. Salvador, J. J. Dannenberg, V. G. Zakrzewski, S. Dapprich, A. D. Daniels, M. C. Strain, O. Farkas, D. K. Malick, A. D. Rabuck, K. Raghavachari, J. B. Foresman, J. V. Ortiz, Q. Cui, A. G. Baboul, S. Clifford, J. Cioslowski, B. B. Stefanov, G. Liu, A. Liashenko, P. Piskorz, I. Komaromi, R. L. Martin, D. J. Fox, T. Keith, M. A. Al-Laham, C. Y. Peng, A. Nanayakkara, M. Challacombe, P. M. W. Gill, B. Johnson, W. Chen, M. W. Wong, C. Gonzalez, and J. A. Pople, *Gaussian 03 (Revision C.02)*, Gaussian, Inc., Wallingford, CT, 2004.
39. K. Sugimori, T. Shuku, A. Sugiyama, H. Nagao, T. Sakurai, and K. Nishikawa, *Polyhedron*, 2005, **24**, 2671–2675.
40. N. Kitajima, K. Fujisawa, C. Fujimoto, Y. Morooka, S. Hashimoto, T. Kitagawa, K. Toriumi, K. Tatsumi, and A. Nakamura, *J. Am. Chem. Soc.*, 1992, **114**, 1277–1291.
41. Bruker, *APEXII*, Bruker AXS Inc., Madison, WI, USA, 2005.
42. *SADABS and SAINT*, Bruker AXS Inc., Madison, WI, USA, 2003.
43. G. M. Sheldrick, *Acta Cryst.*, 2008, **A64**, 112–22.
44. O. V. Dolomanov, L. J. Bourhis, R. J. Gildea, J. A. K. Howard, and H. Puschmann, *J. Appl. Cryst.*, 2009, **42**, 339–42.
45. M. D. Hanwell, D. E. Curtis, D. C. Lonie, T. Vandermeersch, E. Zurek, and G. R. Hutchison, *J. Cheminf.*, 2012, **4**, 17.